

Numerical Modelling of Cross Roll Straightening

A. Mutrux, B. Berisha, B. Hochholdinger, P. Hora
Institute of Virtual Manufacturing, ETH Zurich
CLA F19.3, Tannenstr.3, 8092 Zurich, Switzerland
mutrux@ivp.mavt.ethz.ch

Summary:

The aim of the cross-roll straightening process is to straighten bars having a circular section. To the knowledge of the authors, most of the work published about this process is based on analytical considerations. In the present study, the process is explained and simulated using LS-Dyna. The similarity between three points bending and cross-roll straightening is highlighted. In order to test the straightening ability of the simulation, a bent bar is used as an input for the simulation. Comparing the curvatures of the in- and output bars, it appears that a reduction of the curvature can be predicted.

Keywords:

cross roll straightening, straightness prediction.

1 The cross roll straightening process

1.1 Straightening machines

Metal products – such as bars, rails, and sheets – can be straightened by alternate bending with a decreasing amplitude. Ideally, the last bending step produces such a curvature that, after springback, the product reaches straightness (or flatness). For example, railway rails are straightened by passing through sets of alternate rolls, as depicted in figure (1), where they are reversely bent in one plane.

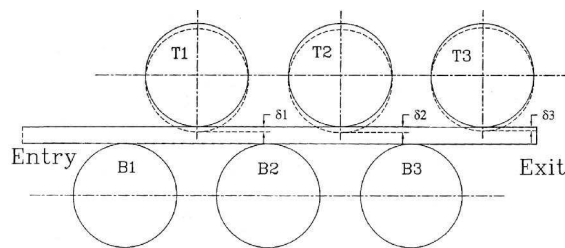


Figure 1: Schematic straightening of railway rails (from [1]).

For bars, the problem is slightly different. Whereas rails tend to bend in one plane due to the different moments of inertia of their section, round bars can bend freely in three dimensions. One solution allowing to straighten such products in space is to bend the material in two planes normal to each other by setting two devices as depicted in figure (1) at a right angle. A characteristic of bars is their ability to be rotated easily around their main axis, even under stress. Based on this fact, another option is to bend the product and make it rotate simultaneously. This second possibility results in processes such as shown in figure (2).

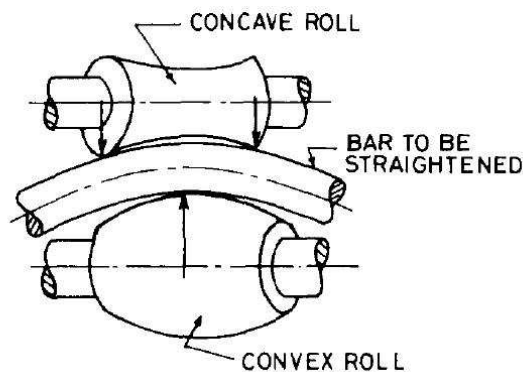


Figure 2: Bar straightening in a cross roll straightening machine (from [2]).

1.2 Deformation path

Figure (2) shows the principle of cross roll straightening – that is the process studied in this paper. The bar passes through two rolls: a concave one and a convex one. As long as the distance between the rolls is larger than the diameter of the bar, the bar undergoes pure bending. For rods having a large diameter, the rolls may also stamp the material – this case is not studied in this paper. Considering a point on the surface of the bar, its path in space is along a helix with a bent axis. As pictured in figure (3), the resulting strain state can be represented as one of a three points bending progressing along a helix. The bending of

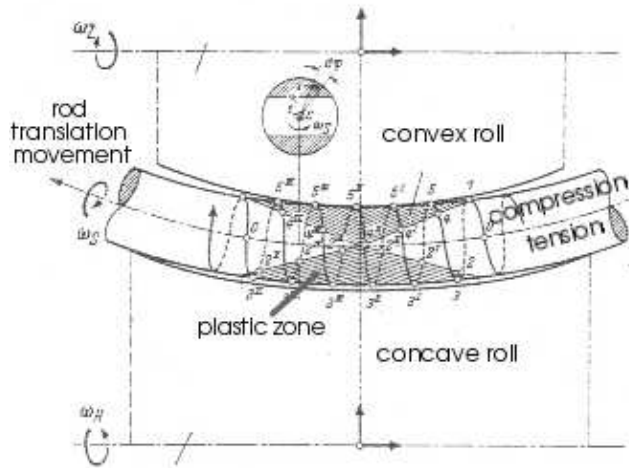


Figure 3: The plastic zone in the bent rod is propagated along a helix (from [5], modified).

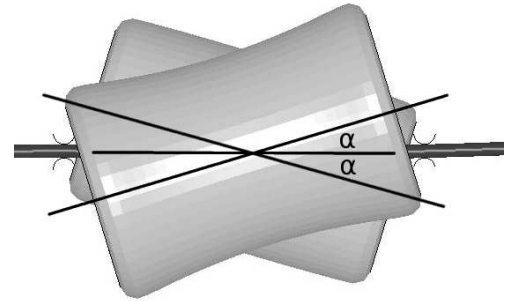


Figure 4: The angle α between the rolls and the bar.

the bar can be controlled by varying the angle α between the rolls and the bar (see figure (4)): the smaller the α , the more bending occurs. The optimal α is such that the highest straightness of the bar is reached while still having an economically realistic translation speed. Nowadays, the choice of α is made mostly on an empirical basis.

Analytical approaches of the straightening process can be found in the references (particularly [4] and [6]). Nevertheless, these approaches are based on numerous more or less offhand hypotheses. To the knowledge of the authors, most of the research done about cross roll straightening was done during the pre-simulative era. A deeper understanding of the process is expected through the use of LS-Dyna.

1.3 Bending simulation

As mentioned above, cross roll straightening is a repetitive bending process. Before simulating the whole cross roll straightening process – with the rotating rolls – a simulation is made where the rod is simply bent by the closing of the rolls. Figure (5) shows the stress distribution of the upper elements (in contact with the concave roll) of the bar during bending as a function of their position along the bar axis. The simulation parameters are the same as for the cross rolling simulation described below. Only the elements in the middle of the bar reach plastic deformation. As it will be shown later, the stress distribution obtained corresponds to the stress envelope of an element passing through the rolls in the full cross roll simulation.

2 The simulation of the cross roll straightening process

2.1 Geometry

In figure (6), one can see the different parts of the model. The rod itself – meshed with fully integrated (type 2) volume elements – is number 1. Part 2 is modelled with beams and represents the extension of the rod. These beam elements are never in contact with the rolls: their sole purpose is to give the rod a realistic

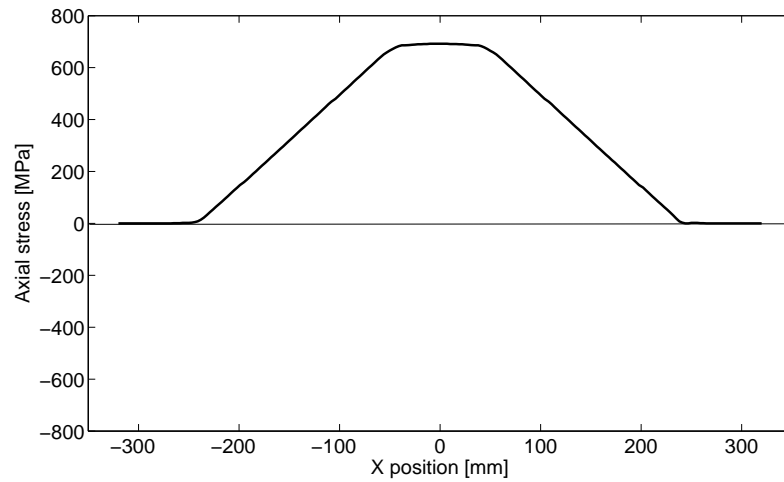


Figure 5: Axial stress of the elements in contact with the concave roll during the closing of the rolls (simple three points bending simulation) as a function of their position along the bar axis.

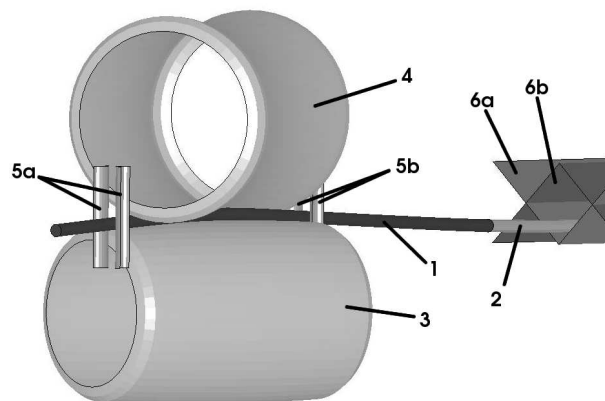


Figure 6: The different parts of the model. The rod (part No 1) moves from right to left as the rolls (parts No 3 and 4) rotate.

behaviour during both the gravity and the rolling operations by remaining in the box defined by parts 6a and 6b. The beams are fixed to the rest of the bar using a *CONSTRAINED_NODAL_RIGID_BODY. Parts 3 and 4 are, respectively, the convex and concave rolls: both meshed with shell elements and considered as rigid bodies. The guides 5a and 5b, also rigid bodies, keep the rod in place during the whole simulation.

2.2 Process

The simulation is divided in three main steps:

1. **gravity**: the rod falls on the convex roll due to gravity.
2. **closing**: the rolls close and bend the bar.
3. **rolling**: the rolls rotate – this operation is the 'core' of the process.

The rod considered in the simulation is 10 [m] long: 1.5 [m] is meshed with volume elements and the rest is discretised with beams. This avoids, using a technique quite close to reality, extra constraints to appear in the rod due to the oscillation of the bar. The main drawback of this method is that the **gravity** operation has to be long enough before the bar stops swinging in the box. To reduce computation time, a mixed time integration strategy is chosen: the **gravity** is computed with the 'implicit' flag turned on and the rest of the simulation is integrated explicitly.

After the **gravity** step, the **closing** of the rolls takes place, during which the concave roll is translated towards the convex one, bending the bar. Once, the bar is bent, the proper **rolling** takes place. During **rolling**, the only loads applied are the ones induced by the rigid body rotations of the rolls. The contact between the rolls and the rod is done with the _SMOOTH option turned on, thus allowing to use a reduced number of elements to model the rolls.

2.3 Material behaviour

Compression-tension tests have been done on the material to be straightened – the results can be seen in figure (7). One observes a different yield stress for the second part of the deformation (the tensile deformation). This difference in yield stress can be explained by the kinematic hardening behaviour of the material. In cross-roll straightening, the material also undergoes reverse loading – an isotropic material model would necessarily be a major simplification. For the present simulation, a purely kinematic hardening model is fitted to the experimental data (*MAT_PLASTIC_KINEMATIC). Future work shall include a more complex kinematic behaviour, such as the model proposed by Chaboche [10].

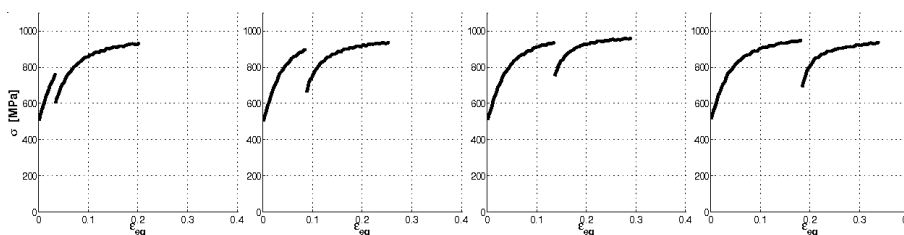


Figure 7: Different plastic pre-straining in compression with a subsequent tension loading

2.4 Simulation results

The stress state obtained is uniaxial – radial stresses do not exceed 10 [Mpa]. The general shape of the axial stress on one element (see figure (8)) corresponds to what one would have expected after seeing figure (5). From the theoretical pitch of the helix mentioned above: $p = 2\pi r \tan(\alpha) \approx 24$ [mm] (for $r = 12.5$ [mm] and $\alpha = 17$ [deg]) and knowing that the distance between the three contact points in the simulation is about 480 [mm], the number of peaks should be $480/24 = 20$. As can be seen in figure (8), there are about 10 peaks in the first part of the straightening itself.

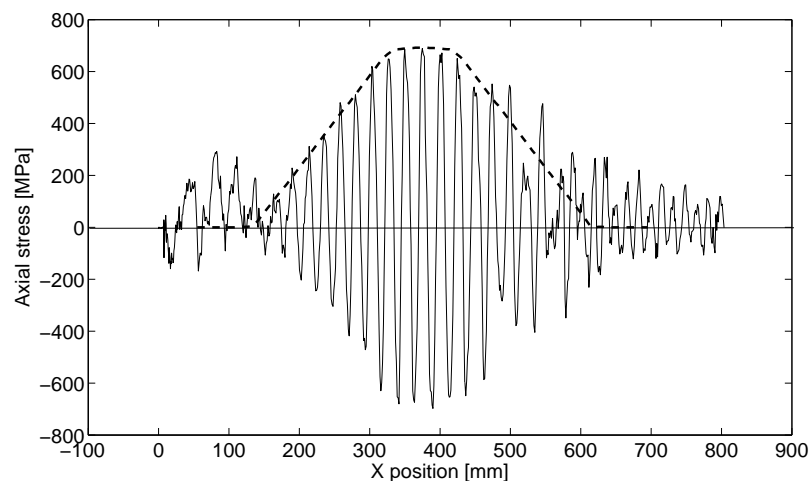


Figure 8: Axial stress acting on an element on the outer layer of the rod as a function of its position between the rolls. The stress envelope corresponds to the stress distribution obtained in bending.

Concerning the smaller stress peaks outside the envelope, a possible explanation is the swinging of the rod when it is not in the rolls. The stress envelope plotted in figure (8) is only a translation in X of the results plotted in figure (5). The good agreement between the stress peaks from the rolling simulation and the stress distribution from the bending simulation prove the validity of the assumption mentioned earlier: the reduction of the cross rolling simulation to a series of alternate bendings. In the second part of the graph (after the maximum stress peak), one can observe a discrepancy between the two curves. This phenomenon may be explained by the fact that, in the bending simulation, the elements on the right hand side have no deformation history – they have not been bent back and forth. In order to account precisely for a kinematic hardening behaviour of the material, the whole process has to be simulated.

3 The straightening effect prediction

In order to test the straightening ability of the model, a curved bar with a radius of curvature (in a single plane) about 9400 [mm] is used as an input. The definition of straightness is normally related to an axial length, typically the maximum deviation from a perfect line on 1 [m]. Applying such a criterion to the present problem would require simulating the process with very long bars, which would lead to excessive computation times. To circumvent this problem, the straightness of the product is defined through its curvature in the middle of a 100 [mm] rod segment. Nodes on the middle axis of the rod are taken as references and a plane is fitted across them. On the fitted plane, a two-dimensional coordinate system is built, from which a parabola is fitted through the points. The second derivative of the parabola corresponds to the local curvature of the rod. The adequate number of points to be taken for the fit is a delicate issue.

If too few points are taken, numerical errors gain greater importance. But, as the output rod has generally a three dimensional curvature, the more nodes are taken, the farther they are from the fitted plane, which also induces errors. Therefore, the number of nodes to be taken depends on the curvature with which one has to deal: a few trials are recommended.

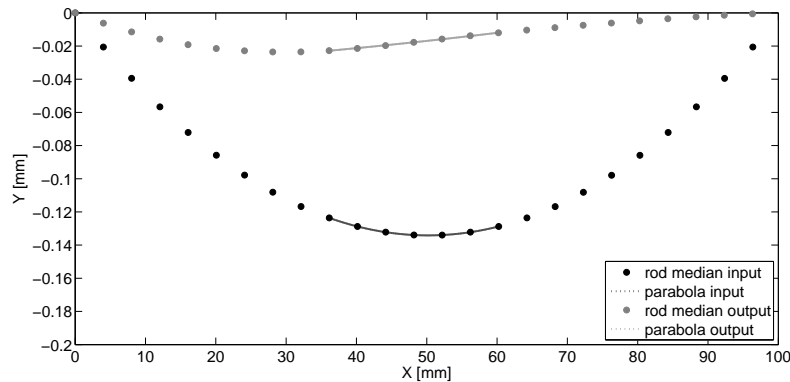


Figure 9: Parabola fitted to in- and output nodes from the median line of the rod in the XY plane.

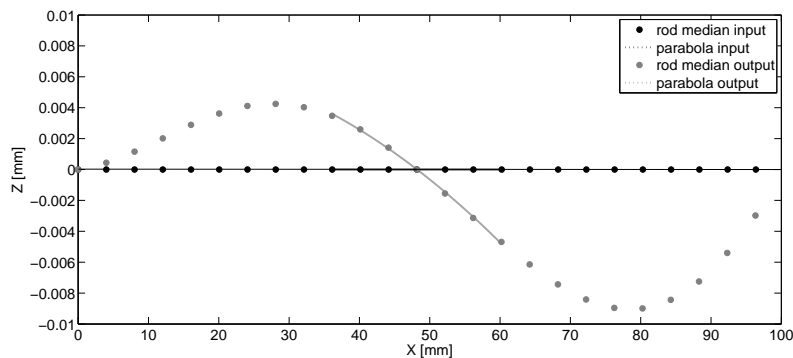


Figure 10: In- and output rod curvatures in the XZ plane.

Figures (9) and (10) show the rod curvature before and after the straightening process. As it can be seen, whereas the input rod is only curved in one plane, the curvature of the output rod is three-dimensional. In the example taken, the radius of curvature of the bar after straightening is about $100 \cdot 10^3$ [mm].

4 Summary

Based both on workshop observations and on the references below, a cross-roll straightening device has been simulated. The similitude between the stress state obtained in three points bending and in cross-roll straightening has been highlighted. By passing through the rolls, the curvature of a bent bar can be significantly reduced.

The kinematic hardening behaviour of the material is to be more precisely investigated. In the simulation presented here, a simple linear hardening kinematic is used. Future work shall consider more complex hardening models.

References

- [1] Srimani, S.L. and Basu, J. An investigation for control of residual stress in roller-straightened rails, *J. Strain Analysis*, Vol. 38, No.3 , 2003, 261–268
- [2] Das Talukder, N.K. and Johnson, W. On the arrangement of rolls in cross-roll straighteners, *Int. J. Mech. Sci.*, Vol. 23, 1981, 213–220
- [3] Das Talukder, N.K and Singh, A.N. Mechanics of bar straightening, Part 1: general analysis of straightening process, *Trans. A.S.M.E.*, Vol. 113, 1991, 224–227
- [4] Das Talukder, N.K and Singh, A.N. Mechanics of bar straightening, Part 2: straightening in cross-roll straighteners, *Trans. A.S.M.E.*, Vol. 113, 1991, 228–232
- [5] Fangmeier, R. Untersuchungen über das Richten von Rundstäben in zwei-Walzen-Richtmaschinen, *Doctoral Thesis, Technischen Hochschule Claustahl*, 1966
- [6] Yu, T.X. and Johnson, W. Estimating the curvature of bars after cross roll straightening, *Proc. 22nd Int. Machine Tool Des. and Res. Conf. (MTDR), Manchester, UK*, 1981, 517–521
- [7] Yu, T.X. and Zhang, L.C. Plastic bending: theory and applications, *World Scientific Publishing*, USA, 1996
- [8] Wu, B.J. and Chan, L.C. A study on the precision modeling of the bars produced in two cross-roll straightening, *J. Materials Processing Technology*, 2000, 202–206
- [9] Schleinzer, G. and Fischer, F.D. Residual stresses in new rails, *J. Materials Science and Engineering*, 2000, 280–283
- [10] Chaboche, J.L. Constitutive equations for cyclic plasticity and cyclic viscoplasticity, *Int. J. Plasticity*, Vol. 5, 1989, 247–302